J Mol Model (2011) 17:2151–2157
DOI 10.1007/s00894-010-0836-z

ORIGINAL PAPER

Molecular surface electrostatic potentials as guides to Si-O-N angle contraction: tunable σ-holes

Jane S. Murray · Monica C. Concha · Peter Politzer

Received: 2 August 2010 / Accepted: 23 August 2010 / Published online: 26 September 2010

Abstract We have demonstrated that the variation in the experimentally-determined Si-O-N angles in XYZSi-O-N $(CH_3)_2$ molecules, which depends upon the positions and natures of the substituents X, Y and Z, can be explained in terms of computed electrostatic potentials on the molecular surfaces of the corresponding XYZSi-H molecules. The latter framework has been used as a model for what the nitrogen lone pair in the XYZSi-O-N$(CH_3)_2$ molecules sees. Both optimized geometries and electrostatic potentials of our model XYZSi-H systems have been obtained at the B3PW91/6-31G(d,p) level. We propose that the driving force for the observed Si-O-N angle contraction in XYZSi-O-N$(CH_3)_2$ molecules is largely the electrostatic attraction between a positive σ-hole on the silicon and the lone pair of the nitrogen. Negative regions that may be near the silicon σ-hole, arising from substituents with negative potentials, also play an important role, as they impede the approach of the nitrogen lone pair. These two factors work in synergy and attest to the electrostatically-driven nature of the Si–-N intramolecular interactions, highlighting their tunability.

Keywords Electrostatic potentials · Intramolecular interactions · Si-O-N angles · σ-hole interactions · Tunability

J. S. Murray (✉) · P. Politzer
CleveTheoComp LLC,
1951 W. 26th Street,
Cleveland, OH 44113, USA
e-mail: jsmurray@uno.edu

M. C. Concha
Department of Chemistry, University of New Orleans,
New Orleans, LA 70148, USA

Introduction

Mitzel et al. have synthesized and characterized, both experimentally and computationally, an interesting series of molecules containing the Si-O-N$(CH_3)_2$ linkage [1–7]. A prototypical XYZSi-O-N$(CH_3)_2$ molecule, **1**, is shown below. Note that in **1a**, X is *anti* to the nitrogen (X, Si, O and N are essentially coplanar), and Y and Z are *gauche* to it, while in **1b**, Y is *anti* to the nitrogen, and X and Z are *gauche*. These molecules exhibit relatively small Si-O-N

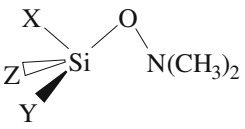

1a

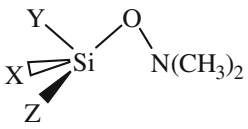

1b

angles, in the range 75° to 110° [1–7], compared to the isoelectronic Si-O-CH$(CH_3)_2$ linkage [1, 8], approximately 125°. The extent of the Si-O-N angle contraction has been found to be dependent upon the natures of the X, Y and Z substituents and their orientations relative to the nitrogen [1–7]. The reason for this angle contraction has been a matter of some controversy, as has the nature of the interaction between the nitrogen and the silicon in these molecules [1–7, 9–11]. For example, Kostyanovskii and Prokov'ev suggested the presence of a dative bond between silicon and nitrogen [9], while Mitzel et al. concluded more recently that both computational and experimental evidence point to electrostatics and dipole forces as being key factors [3, 5].

Table 1 lists experimentally-determined Si-O-N bond angles and S–-N internuclear distances for a series of these molecules. Note that the solid state Si-O-N angles and

Table 1 Experimentally-determined Si-O-N bond angles and Si–-N internuclear distances for a series of XYZSi-O-N$(CH_3)_2$ molecules

Molecule	X-Ray diffraction		Gas phase electron diffraction		Reference
	Si-O-N angle (degrees)	Si—N (Å)	Si-O-N angle	Si—N	
4b, Cl_2HSi-O-N$(CH_3)_2$ (2 Cl's *gauche*)			111.1(20)		6
5, Cl_3Si-O-N$(CH_3)_2$	103.4(1)	2.441(2)	105.6(8)	2.473(12)	4
	102.6(1)	2.432(2)			4
2, H_3Si-O-N$(CH_3)_2$	102.63(5)	2.453(1)			2
3b, ClH_2Si-O-N$(CH_3)_2$ (Cl *gauche*)			104.7(11)	2.468(25)	3
4a, Cl_2HSi-O-N$(CH_3)_2$ (1 Cl *anti*, 1 Cl *gauche*)			98.8(12)		6
3a, ClH_2Si-O-N$(CH_3)_2$ (Cl *anti*)	79.7(1)	2.028(1)	87.1(9)	2.160(7)	3
6, F_3Si-O-N$(CH_3)_2$	77.1(1)	1.963(1)	94.3(9)	2.273(17)	5
7b, $(F_3C)F_2Si$-O-N$(CH_3)_2$ (CF_3 *gauche*)			87.8(20)	2.174	7
7a, $(F_3C)F_2Si$-O-N$(CH_3)_2$ (CF_3 *anti*)	74.1(1)	1.904(1)	84.4(32)	2.112	7

Si–-N distances are in every case smaller than the gas phase (for the molecules for which both are available). When X, Y and Z are the same, as in H_3Si-O-N$(CH_3)_2$, F_3Si-O-N$(CH_3)_2$ and Cl_3Si-O-N$(CH_3)_2$, there is no possibility for *anti* and *gauche* conformers. However, for ClH_2Si-O-N$(CH_3)_2$, HCl_2Si-O-N$(CH_3)_2$ and $(F_3C)F_2Si$-O-N$(CH_3)_2$, two conformers of each are possible. The angle contraction is greater in these when Cl or CF_3 is in the *anti* position relative to the nitrogen rather than the *gauche* [3, 6, 7].

Our purpose in this paper is to demonstrate that the degree of angle contraction in XYZSi-O-N$(CH_3)_2$ systems can be related to the electrostatic potentials on the surfaces of the corresponding XYZSi-H molecules. A key factor is the presence of positive σ-holes, on the covalently-bonded tetravalent silicon atoms [12–14].

A σ-hole is simply the electron deficiency that is associated with the formation of a σ-bond; this deficiency is on the side of the atom away from the bond, along its extension. This is usually accompanied by a region of positive electrostatic potential through which the atom can interact, in a highly directional manner, with negative sites. The presence of positive σ-holes was used by Clark et al. [15] initially to explain the occurrence of halogen bonding [15–19], but they can be found as well on covalently-bonded atoms of Groups IV-VI [12–14, 20–23], and even, we suggest, hydrogen [19, 24]. σ-Holes are most easily identified by the molecular electrostatic potential [12–25], as will be discussed in the next section. For an overview of σ-hole bonding, see Politzer and Murray [25].

Molecular electrostatic potentials

The electrostatic potential V(**r**) created at the point **r** by the nuclei and electrons of an atom or molecule is given by Eq. 1:

$$V(\mathbf{r}) = \sum_A \frac{Z_A}{|\mathbf{R}_A - \mathbf{r}|} - \int \frac{\rho(\mathbf{r}')d\mathbf{r}'}{|\mathbf{r}' - \mathbf{r}|}, \quad (1)$$

Z_A is the charge on nucleus A, located at $\mathbf{R}_A$, and ρ(**r**) is the electronic density function. The first term on the right side of Eq. 1 is due to the nuclei and is positive; the second reflects the contribution of the dispersed electrons and is negative. The sign of V(**r**) in any particular region of space is dependent upon which term on the right side of Eq. 1 is dominant there.

The electrostatic potential was introduced into chemistry in the 1970s [26] to provide a nonarbitrary means of assessing which regions of space around a molecule are more positive or more negative. V(**r**) is a local property and is a physical observable, which can be determined experimentally as well as computationally [27, 28]. An important feature of the electrostatic potential is that it shows very clearly that atoms in molecules sometimes have regions of both positive and negative V(**r**) [29], and thus can interact electrostatically with both negative and positive sites. This highlights one of the problems associated with assigning a single positive or negative charge to an atom in a molecule [19, 29, 30].

The electrostatic potential V(**r**) has been shown to be extremely effective in analyzing noncovalent interactions [30]. For such applications, it is useful to plot V(**r**) on an appropriate outer surface of the molecule [31]. Following Bader et al. [32], we choose this to be the 0.001 au (electrons/bohr^3) contour of the electronic density; V(**r**) computed on this surface is labeled $V_S(\mathbf{r})$. The most positive and the most negative sites on the molecular surface are designated $V_{S,max}$ and $V_{S,min}$, respectively; there may be several local $V_{S,max}$ and $V_{S,min}$ on a given molecular surface. It has been shown that hydrogen $V_{S,max}$ and basic site $V_{S,min}$

correlate well with empirical measures of hydrogen-bond-donating and -accepting tendencies [33]. It has further been demonstrated that a number of condensed phase physical properties that depend upon noncovalent interactions can be related analytically to statistically-defined features of $V_S(\mathbf{r})$, such as its average deviation, positive and negative variances, etc. [34]. These properties include enthalpies of phase transitions, solubilities and solvation energies, boiling temperatures and critical constants, etc.

An important type of noncovalent interaction is σ-hole bonding [25], mentioned in the Introduction. This involves regions of positive potential on covalently-bonded Group IV – VII atoms interacting attractively, in a highly directional manner, with negative sites on other molecules (or even within the same one) [12–25]. We and others have shown that such positive regions are often found on the extensions of the covalent bonds to these atoms; they typically result from the electron deficiency in the outer lobe of a half-filled *p*-type bonding orbital that is participating in a σ bond. A σ-hole is more positive as the partner in the covalent bond is more electron-withdrawing. Thus, as shall be seen, the silicon σ-hole on the extension of a Cl-Si bond is more positive than that on the extension of an H-Si bond [12].

Riley et al. [18] have shown that the $V_{S,max}$ associated with the σ-holes in a series of brominated benzenes and pyrimidines correlate with their interaction energies with acetone. The electrostatic nature of σ-hole interactions is further demonstrated by the work of Shields et al. [24].

Computational approach

In using molecular surface electrostatic potentials to analyze and predict noncovalent interactions, e.g., A–-B, it is necessary to look at the $V_S(\mathbf{r})$ of A and B separately, *prior* to interaction. This will reveal the regions of positive and negative $V_S(\mathbf{r})$ on A and on B through which attraction can occur. These will not be evident in the $V_S(\mathbf{r})$ of the complex A–-B, because they will have been neutralized by the interaction [35–37].

In the present project, the grouping $O\text{-}N(CH_3)_2$ is common to all of the molecules being considered (Table 1). We shall therefore focus upon the $V_S(\mathbf{r})$ of the XYZSi portions, as modeled by XYZSi-H molecules. We will look specifically at the $V_S(\mathbf{r})$ of the silicon atoms and their immediate environments, since these are in closest proximity to the nitrogens of the $O\text{-}N(CH_3)_2$ groupings.

We have obtained optimized structures for a series of XYZSi-H molecules at the B3PW91/6-31G(d,p) level using Gaussian 09 [38]. We then computed the 0.001 au surface electrostatic potentials using the WFA-Surface Analysis Suite [31]. The latter allows us to identify the $V_{S,max}$ and $V_{S,min}$ associated with these molecules, as well as to create graphical visualizations of $V_S(\mathbf{r})$.

The XYZSi-H molecules for which we have determined $V_S(\mathbf{r})$ are listed in Table 2. These were chosen to mimic the XYZSi portions of the $XYZSi\text{-}O\text{-}N(CH_3)_2$ molecules in Table 1, for which experimental X-ray diffraction and/or gas phase electron diffraction structural data are tabulated.

Results and discussion

Figures 1 and 2 show $V_S(\mathbf{r})$ for $H_3Si\text{-}H$ and $ClH_2Si\text{-}H$. Striking features of each are the regions of positive electrostatic potential on the silicons along the extensions of the H-Si and Cl-Si bonds. These regions reflect the deficiencies of electron density that have been labeled σ-holes, through which highly-directional interactions with negative sites can take place. For example, such positive regions on silicon have been identified as the driving force for the formation of SiF_4 complexes with amines [13].

Table 2 Computed surface electrostatic potential maxima ($V_{S,max}$) and minima ($V_{S,min}$) for a series of XYZSi-H molecules, where X, Y and Z are H, F, Cl or CF_3. Only $V_{S,max}$ on the silicons are listed; these correspond to their respective σ-holes. Electrostatic potentials are in units of kcal mol^{-1}

Molecule	Bond producing σ-hole	$V_{S,max}$ on Si[a]	$V_{S,min}$
$H_3Si\text{-}H$	H-Si	13.0 (4)[b]	none[b]
$Cl_3Si\text{-}H$	Cl-Si	26.2 (3)	Cl: –5.3
	H-Si	17.4 (1)	
$HCl_2Si\text{-}H$	Cl-Si	29.6 (2)	Cl: −9.7
	H-Si	19.5 (2)	
$H_2ClSi\text{-}H$	Cl-Si	31.0 (1)[b]	Cl: −12.9[b]
	H-Si	17.7 (3)[b]	
$F_3Si\text{-}H$	F-Si	36.3 (3)	
	H-Si	31.1 (1)	F: −12.4
$(F_3C)F_2Si\text{-}H$	F_3C-Si	38.4 (1)	F(Si): −10.2
	F-Si	35.8 (2)	$F(CF_3)$: −7.5, −7.0, −7.0
	H-Si	30.3 (1)	

[a] The number of $V_{S,max}$ on the silicon with the same value are given in parentheses

[b] This value is from reference [12]

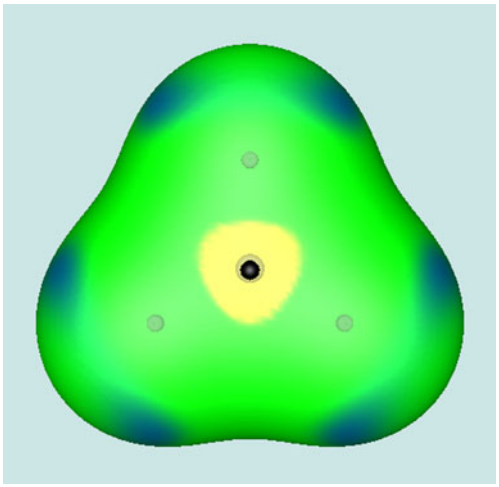

Fig. 1 Computed electrostatic potential on the 0.001 au molecular surface of H_3Si-H. The black hemisphere indicates the location of the σ-hole $V_{S,max}$ on the extension of one of the H-Si bonds. Color ranges, in kcal mol^{-1}, are: red, greater than 20.0; yellow, between 20 and 10; green, between 10 and 0; blue, less than zero (negative)

Compare the $V_S(\mathbf{r})$ of H_3Si-H shown in Fig. 1 with that of ClH_2Si-H in Fig. 2a. In the former, we are looking at the σ-hole $V_{S,max}$ on the extension of one of the four H-Si bonds; its value is 13.0 kcal mol^{-1} (Table 2). In Fig. 2a, we are looking at the $V_{S,max}$ on the extension of the Cl-Si bond in ClH_2Si-H, which has a value of 31.0 kcal mol^{-1}. Apart from the difference in magnitudes of the $V_{S,max}$, the views are similar in that they display regions of the molecules that are totally dominated by positive electrostatic potentials. In proceeding to Fig. 2b, in which the view is along the extension of one of the H-Si bonds, this picture changes. There is again a positive region with a σ-hole $V_{S,max}$ on the extension of the H-Si bond, with a magnitude of 17.7 kcal mol^{-1}, but there is also visible a region of negative $V_S(\mathbf{r})$ associated with the lateral sides of the chlorine.

It was pointed out in the Introduction that the Si-O-N angles in XYZ-Si-O-$N(CH_3)_2$ molecules (Table 1) are significantly less than the Si-O-C angles in isoelectronic XYZ-Si-O-$CH(CH_3)_2$ systems, which are approximately 125°. We propose that the driving force for the Si-O-N contraction is largely the electrostatic interaction between a positive σ-hole on the silicon and the lone pair of the nitrogen. It is particularly the σ-hole corresponding to the bond that is *anti* to the nitrogen that is significant, since this is the one that faces the nitrogen lone pair.

Let's consider Figs. 1 and 2 in relation to the Si-O-N angles found experimentally in H_3Si-O-$N(CH_3)_2$ (**2**) and the *anti* and *gauche* conformers of ClH_2Si-O-$N(CH_3)_2$ (**3a** and **3b**). In the solid state, the Si-O-N angles in **2** and **3a** are 102.63(5)° [2] and 79.7(1)° [3], respectively.

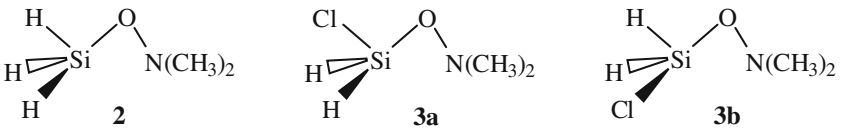

This suggests a stronger attraction between the nitrogen and silicon atoms in **3a** than in **2**, and this is confirmed by the computed $V_S(\mathbf{r})$. The nitrogen lone pair in **3a** is facing a positive region similar to that seen in Fig. 2a, which has a $V_{S,max}$ of 31.0 kcal mol^{-1}, whereas the nitrogen in **2** is interacting with a $V_S(\mathbf{r})$ like that in Fig. 1, which has $V_{S,max}$=13.0 kcal mol^{-1}. The attractive interaction in **3a** is consequently stronger.

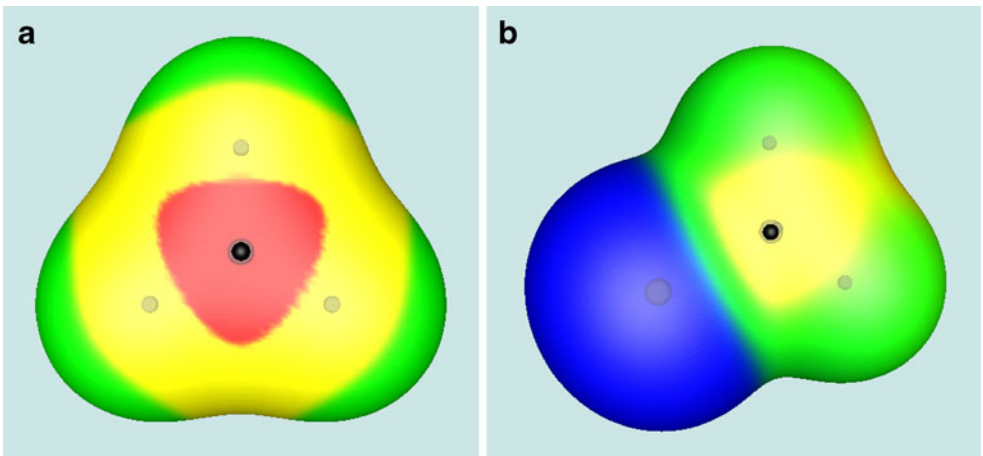

Fig. 2 Computed electrostatic potential on the 0.001 au molecular surface of ClH_2Si-H. Two views are shown: (**a**) chlorine is behind the plane of the paper; (**b**) chlorine is to the left. The black hemispheres indicate the locations of the σ-hole $V_{S,max}$ corresponding to (**a**) the Cl-Si bond, and (**b**) an H-Si bond. Color ranges, in kcal mol^{-1}, are: red, greater than 20.0; yellow, between 20 and 10; green, between 10 and 0; blue, less than zero (negative)

Table 3 Computed surface electrostatic potential maxima ($V_{S,max}$) and minima ($V_{S,min}$) for mono-, di- and tricyanosilane. Only $V_{S,max}$ on the silicons are listed; these correspond to their respective σ-holes. Electrostatic potentials are in units of kcal mol^{-1}

Molecule	Bond producing σ-hole	$V_{S,max}$ on Si[a]	$V_{S,min}$
$(NC)H_2Si$-H	NC-Si	34.1 (1)	N: −35.1
	H-Si	25.0 (3)	
z$(NC)_2HSi$-H	NC-Si	42.9 (2)	N: −28.4
	H-Si	34.9 (2)	
$(NC)_3Si$-H	NC-Si	49.7 (3)	N: −22.9
	H-Si	42.2 (1)	

[a] The number of $V_{S,max}$ on the silicon with the same value are given in parentheses

What about the *anti* and *gauche* conformers of ClH_2Si-O-$N(CH_3)_2$, **3a** and **3b**? For these, we can compare the gas phase electron diffraction data that are available (Table 1). The Si-O-N angles for the *anti* and *gauche* conformers are 87.1(9)° and 104.7(11)°, respectively [3]. The degrees of angle contraction in these two conformers are consistent with the views of $V_S(\mathbf{r})$ shown in Fig. 2a and b. In **3a**, the nitrogen sees the $V_S(\mathbf{r})$ in Fig. 2a, with its $V_{S,max}$ of 31.0 kcal mol^{-1}. In **3b**, however, the nitrogen faces the potential in Fig. 2b, which has a weaker $V_{S,max}$ of 17.7 kcal mol^{-1}. In addition, in **3b**, the nitrogen lone pair will feel some repulsion due to the negative lateral side of the chlorine, Fig. 2b; this repulsion does not occur when the nitrogen lone pair interacts with the $V_S(\mathbf{r})$ shown in Fig. 2a.

The cases of H_3Si-O-$N(CH_3)_2$ (**2**) and the two conformers of ClH_2Si-O-$N(CH_3)_2$, **3a** and **3b**, illustrate two factors that help to determine the degree of Si-O-N angle contraction in XYZSi-O-$N(CH_3)_2$ molecules: (1) the strength of the positive σ-hole that faces the nitrogen, which is the one on the extension of the bond to the *anti* substituent, and (2) the presence or absence of negative regions adjacent to this positive region. In Figs. 1 and 2a, we see that the positive σ-hole is stronger in the latter, and that in neither case is there visible a negative region. Thus, the relative Si-O-N angle contractions in **2** and **3a** can be predicted from the strengths of the σ-holes alone. However, in Fig. 2b, both the positive σ-hole and the negative region on the chlorine are facing the nitrogen. So in **3b**, the Si-O-N angle contraction represents a balance between the attraction of the nitrogen lone pair for the positive σ-hole and the repulsion between the lone pair and the negative side of the chlorine.

We proceed now to the two conformers of Cl_2HSi-O-N$(CH_3)_2$, **4a** and **4b**. In **4a**, one chlorine is *anti* to the nitrogen and the other is *gauche*, while in **4b** both chlorines are *gauche* to the nitrogen. The gas phase Si-O-N angles in **4a** and **4b** were reported to be 98.8(12)° and 111.1(20)°, respectively [6] (Table 1). To understand these angles, we look at the surface electrostatic potential of Cl_2HSi-H.

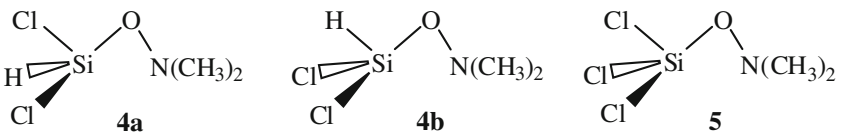

Figure 3a and b show what the nitrogen lone pair "sees" in **4a** and **4b**. The positive region of electrostatic potential in Fig. 3a, corresponding to the σ-hole along the extension of a Cl-Si bond, is stronger than that in Fig. 3b, which is due to the σ-hole along the extension of an H-Si bond, 29.6 *vs*. 19.5 kcal mol^{-1} (Table 2). In addition, the lone pair encounters more negative potential in Fig. 3b, which has a repulsive effect. The net result of these two factors, the strength of the positive σ-hole on the silicon and the existence of regions of negative potential, yields a more contracted angle for **4a** than for **4b**.

That the Si-O-N angle of **4a** is greater than that of **3a** can also be rationalized on this basis. A nitrogen interacting with the face of ClH_2Si-H shown in Fig. 2a "sees" a region of space devoid of negative electrostatic potential; however on the side of Cl_2HSi-H shown in Fig. 3a, the nitrogen encounters both a positive σ-hole and a negative region due to a chlorine.

What about the angle contraction in Cl_3Si-O-$N(CH_3)_2$, **5**? In the solid state, the Si-O-N angle of **5** is very similar to that of H_3Si-O-$N(CH_3)_2$, **2**. This may seem surprising, since the σ-holes due to the Cl-Si bonds in Cl_3Si-H are twice as strong as those from the H-Si bonds in H_3Si-H, 26.2 *vs*. 13.0 kcal mol^{-1} (Table 2). However the nitrogen lone pair in **5** must also contend with the repulsive effects of the negative regions on the chlorines. The net result is that **2** and **5** have similar Si-O-N angles. The fact that the Si-O-N angle

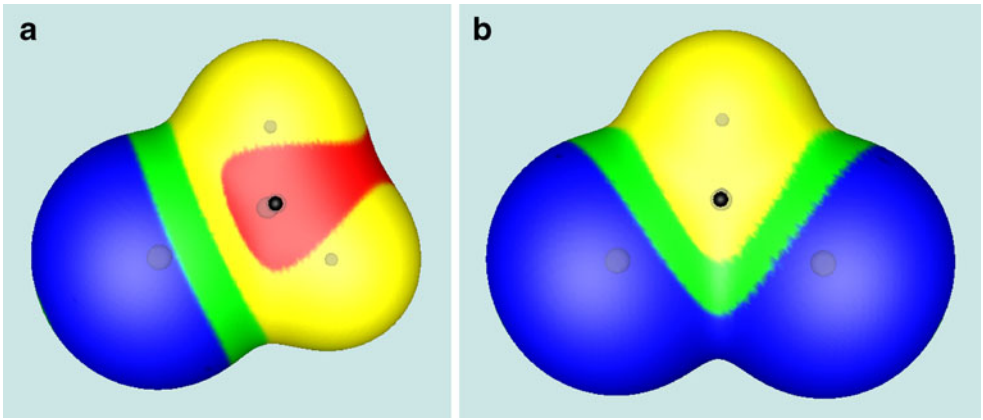

Fig. 3 Computed electrostatic potential on the 0.001 au molecular surface of Cl_2HSi-H. Two views are shown: (**a**) one chlorine is behind the plane of the paper, one is to the left; (**b**) one chlorine is to the left, one is to the right. The black hemispheres indicate the locations of the σ-hole $V_{S,max}$ corresponding to (**a**) a Cl-Si bond, and (**b**) an H-Si bond. Color ranges, in kcal mol^{-1}, are: red, greater than 20.0; yellow, between 20 and 10; green, between 10 and 0; blue, less than zero (negative)

in **5**, which has two *gauche* chlorines and one *anti* chlorine, is smaller than that of **4b** , which has two *gauche* chlorines and one *anti* hydrogen, can be explained by noting in Table 2 that the $V_{S,max}$ associated with the σ-holes on the extensions of the Cl-Si bonds in Cl_3Si-H are greater than those of the H-Si bonds in Cl_2HSi-H.

We look finally at the molecules in Table 1 with the smallest Si-O-N angles, F_3Si-O-N$(CH_3)_2$ (**6**) and the two conformers of $(F_3C)F_2Si$-O-N$(CH_3)_2$, **7a** and **7b**. In **7a** the CF_3 group is *anti* in relation to the nitrogen and in **7b** it is *gauche*. The ordering of their Si-O-N angles from

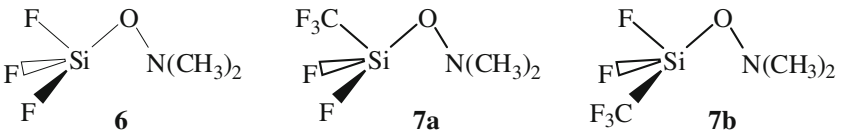

highest to lowest can again be explained by the synergy between (a) the strengths of the σ-hole $V_{S,max}$ on the extensions of the F-Si and F_3C-Si bonds, and (b) the strengths of the negative potentials near these σ-holes (Table 2). Figure 4a and b display the slightly more positive σ-hole potential along the extension of the F_3C-Si bond in $(F_3C)F_2Si$-H compared to the F-Si.

We introduce Table 3 to encourage the synthesis of derivatives of XYZSi-O-N$(CH_3)_2$, where X and/or Y and/or Z are cyano groups. These have the advantage of creating quite positive σ-holes on silicon, along the extensions of the NC-Si bonds, but not having competing negative regions in the immediate proximities of the σ-holes, to impede the approach of the nitrogens toward the silicons.

Summary and perspectives

In this paper, we have demonstrated that the trends in the experimentally-determined Si-O-N angles in XYZSi-O-N

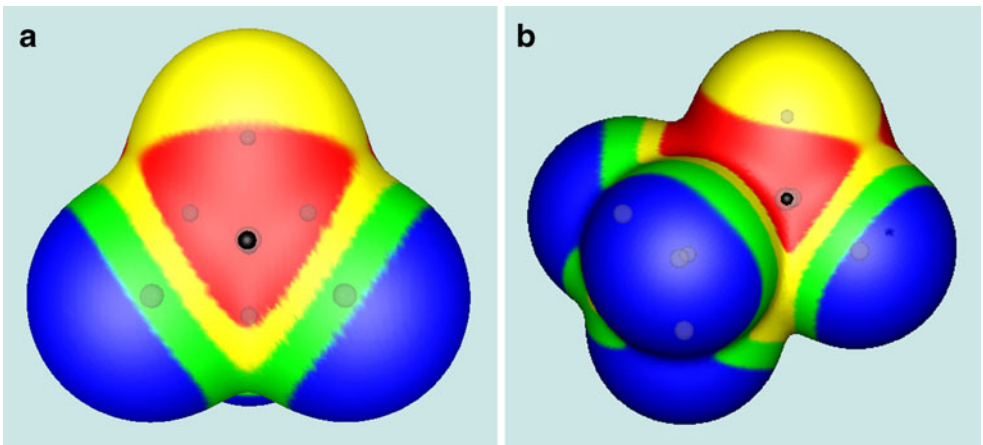

Fig. 4 Computed electrostatic potential on the 0.001 au molecular surface of $(F_3C)F_2Si$-H. Two views are shown: (**a**) CF_3 is behind the plane of the paper; (**b**) CF_3 is to left. The black hemispheres indicate the locations of the σ-hole $V_{S,max}$ corresponding to (**a**) the F_3C-Si bond, and (**b**) an F-Si bond. Color ranges, in kcal mol^{-1}, are: red, greater than 20.0; yellow, between 20 and 10; green, between 10 and 0; blue, less than zero (negative)

$(CH_3)_2$ molecules can be explained by looking at the electrostatic potentials of the corresponding XYZSi-H molecules, which serve as models of what the nitrogen lone pairs are facing. The positions and natures of the substituents X, Y and Z have been shown to be of paramount importance in determining the strengths of the positive σ-hole electrostatic potentials on the silicon. In addition, negative regions near the σ-hole play a role in impeding the approach of the nitrogen lone pair. These two factors work in synergy, resulting in a range of contracted Si-O-N angles in the XYZSi-O-N$(CH_3)_2$ molecules listed in Table 1. Our results attest to the electrostatically-driven nature of the intramolecular interactions between the nitrogen lone pairs and the silicons.

We encourage syntheses that exploit the tunability inherent in systems such as these silicon-containing molecules. This can and should also be utilized in other molecular frameworks having more than one σ-hole on an atom, such as in covalently-bonded atoms of Groups V and VI.

Acknowledgments We thank Professor Andrzej Sokalski and Mrs. Grazyna Sokalska for their help and support in July 2010 in Wroclaw, Poland, without which we would not be submitting this paper.

References

1. Mitzel NW, Blake AJ, Rankin DWH (1997) J Am Chem Soc 119:4143–4148
2. Mitzel NW, Losehand U (1997) Angew Chem Int Ed Engl 36:2807–4148
3. Mitzel NW, Losehand U (1998) J Am Chem Soc 120:7320–7327
4. Losehand U, Mitzel NW, Rankin DWH (1999) J Chem Soc Dalton Trans 4291-4297
5. Mitzel NW, Losehand U, Wu A, Cremer D, Rankin DWH (2000) J Am Chem Soc 122:4471–4482
6. Vojinovic K, Mitzel NW, Foerster T, Rankin DWH (2004) Z Naturforsch 59b:1505–1511
7. Mitzel NW, Vojinovic K, Froehlich R, Foerster T, Robertson HE, Borisenko KB, Rankin DWH (2005) J Am Chem Soc 127:13705–13713
8. Blake AJ, Dyrbush M, Ebsworth EAV, Henderson SGD (1988) Acta Crystallogr C 44:1–3
9. Kostyanovskii RG, Prokov'ev AK (1965) Dokl Akad Nauk SSSR 164:1054–1057
10. Feshin VP, Voronkov MG (1982) J Mol Struct 83:317–320
11. Hagemann M, Mix A, Berger RJF, Pape T, Mitzel NW (2008) Inorg Chem 47:10554–10564
12. Murray JS, Lane P, Politzer P (2009) J Mol Model 15:723–729
13. Politzer P, Murray JS, Lane P, Concha MC (2009) Int J Quantum Chem 109:3773–3780
14. Murray JS, Lane P, Nieder A, Klapötke TM, Politzer P (2010) Theor Chem Acc. doi:10.1007/s00214-009-0723-9
15. Clark T, Hennemann M, Murray JS, Politzer P (2007) J Mol Model 13:291–296
16. Politzer P, Lane P, Concha MC, Ma Y, Murray JS (2007) J Mol Model 13:313–318
17. Politzer P, Concha MC, Murray JS (2007) J Mol Model 13:643–650
18. Riley KE, Murray JS, Politzer P, Concha MC, Hobza P (2009) J Chem Theory Comput 5:155–163
19. Politzer P, Murray JS, Clark T (2010) Phys Chem Chem Phys 12:7748–7757
20. Murray JS, Lane P, Clark T, Politzer P (2007) J Mol Model 13:1033–1038
21. Murray JS, Lane P, Politzer (2007) Int J Quantum Chem 107:2286-2292
22. Clark T, Murray JS, Lane P, Politzer P (2008) J Mol Model 14:689–697
23. Murray JS, Lane P, Politzer P (2008) Int J Quantum Chem 108:2270–2781
24. Shields ZP, Murray JS, Politzer P (2010) Int J Quantum Chem. doi:10.1002/qua.22787
25. Politzer P, Murray JS (2009) In: Leszczynski J, Shukla M (eds) Practical aspects of computational chemistry. Springer, Heidelberg, pp 149–163
26. Scrocco E, Tomasi J (1978) Adv Quantum Chem 11:115–193
27. Stewart RF (1979) Chem Phys Lett 65:335–342
28. Politzer P, Truhlar DG, (eds) (1981) Chemical applications of atomic and molecular electrostatic potentials. Plenum, New York
29. Politzer P, Murray JS, Concha MC (2008) J Mol Model 14:659–665
30. Murray JS, Politzer P (2010) Wiley Interdisciplinary Reviews, in press
31. Bulat FA, Toro-Labbé A, Brinck T, Murray JS, Politzer P (2010) J Mol Model 16(11):1679–1691
32. Bader RFW, Carroll MT, Cheeseman JR, Chang C (1987) J Am Chem Soc 109:7968–7979
33. Hagelin H, Brinck T, Berthelot M, Murray JS, Politzer P (1995) Can J Chem 73:483–488
34. Murray JS, Politzer P (1998) J Mol Struct Theochem 425:107–114
35. Politzer P, Concha MC, Murray JS (2000) Int J Quantum Chem 80:184–192
36. Hussein W, Walker CG, Peralta-Inga Z, Murray JS (2001) Int J Quantum Chem 82:160–169
37. O'Hair RAJ, Williams CM, Clark T (2010) J Mol Model 16:559–565
38. Frisch MJ et al. (2009) Gaussian 09, Revision A1. Gaussian Inc, Wallingford, CT